Precursor Film Profiles of Spreading Liquid Drops

L. Leger,[1] M. Erman,[1,3] A. M. Guinet-Picard,[1] D. Ausserre,[1,a] and C. Strazielle[1,2]
[1]*Physique de la Matière Condensée, Collège de France, 75231 Paris Cedex 05, France*
[2]*Institut Charles Sadron, 67083 Strasbourg Cedex, France*
[3]*Electronique et Physique Appliquée, 94451 Limeil Brévannes, France*
(Received 30 October 1987)

We present the first precise characterization of the profile of the precursor films which progressively develop ahead of the macroscopic edge of a spreading liquid drop. Experiments are performed on a model system (nonvolatile high-molecular-weight polydimethylsiloxane on smooth silicon wafers), using an ellipsometer with a high spatial resolution. Both the film profile and its evolution with time are in good qualitative agreement with recent models which include long-range force effects. Clear quantitative discrepancies may reveal specific polymeric effects.

PACS numbers: 68.10.Gw, 61.25.Hq

A large number of practical situations are conditioned by the wetting of a solid surface by a liquid (paints, textile dying, lubrication, plant nutrition or treatments, metal or glass coating,...). The basic underlying mechanisms are, however, only poorly understood.

We have recently reported experiments on a model system[1]: The spreading of small polydimethylsiloxane (PDMS) droplets deposited on horizontal silicon wafers was followed by observations through a microscope in polarized reflected light, and measurements were made of the size $R(t)$ and of the apparent contact angle $\theta_a(t)$ as a function of time. These experiments clearly demonstrate (1) the universality of the spreading kinetics of the macroscopic part of the drops: $\theta_a(t)$ and $R(t)$ follow scaling laws over more than three time decades, with exponents independent of the spreading parameter $S = \gamma_{SG} - \gamma_{SL} - \gamma$ (γ_{SG}, γ_{SL}, and γ are, respectively, the solid-gas, solid-liquid, and liquid-gas interfacial tension, and S is a measure of the energy, per unit area, gained during the spreading); (2) the existence of a thin precursor film (thickness of a few hundred angstroms or smaller) progressively developing all around the droplets, with a structure strongly dependent on S. All these observations are in qualitative agreement with recent theoretical models by de Gennes and Joanny[2,3] which explicitly take into account the role of long-range forces (for example, van der Waals forces) in the spreading phenomena. Such forces specifically affect the precursor films.

In order to get a better insight into the precursor film behavior and test the validity of these models, we have undertaken film profile determination, on the same model system, using spatially resolved ellipsometry.

The samples are prepared in the following way: A small drop (volume $\Omega \simeq 10^{-7}$ to 10^{-5} cm^3) of liquid PDMS (narrow molecular-weight fractions, $M_w = 6400$, 79000, 160000, and 280000 and $M_w/M_n = 2$, 1.15, 1.11, and 1.19, respectively) is deposited on the polished surface of a silicon wafer. The solid surface, as characterized by ellipsometry and x-ray reflectivity,[4,5] appears to be composed of a 20-Å-thick SiO_2 layer, on top of a Si monocrystal ([111] orientation), with a residual roughness of 4 to 5 Å. In the present Letter we shall only report results obtained on bare wafers ($S > 0$, large), cleaned by oxidation of the surface impurities by uv irradiation under oxygen flow,[6] an efficient cleaning procedure which does not affect the surface roughness. Immediately after the drop deposition, the sample is enclosed in a sealed box, equipped with a glass window, to prevent further contamination by dust or atmospheric impurities during the spreading period which may last for several months. Drop size and apparent contact angle are periodically measured.[1] When the precursor film appears well developed (width larger than 200 μm) by ellipsocontrast microscopic observation,[1] ellipsometric measurements are undertaken. The ellipsometer we use, especially designed to allow for spatial resolution, has already been described.[7,8] We recall here its characteristics relevant for the present investigation: The incident wavelength is set at $\lambda_0 = 0.414$ μm in order to maximize the film contrast on silicon; the angle of incidence is $\alpha_0 = 66°$, slightly out of Brewster's incidence to allow for a finite beam aperture. The incident polarizer is fixed; the intensity of the outcoming reflected beam, monitored after a rotating analyzer, is numerically Fourier transformed. The reflectivity of the system is characterized through the two ellipsometric parameters Δ and ψ defined by $r_\parallel / r_\perp = \tan\psi e^{i\Delta}$, with $r_\parallel$ and $r_\perp$ the reflection coefficients in and normal to the plane of incidence.[9] $\cos\Delta$ and $\tan\psi$ are extracted from the amplitude and the phase of the intensity component modulated at the rotation frequency of the analyzer.[8] The light source is imaged on the sample, where the size of the illuminated spot can be decreased down to 10×25 μm^2. The sample can be swept horizontally and vertically by two-step motor micropositioning devices, with a 10-μm resolution.

Typical $\cos\Delta$ and $\tan\psi$ curves for a sweep through a PDMS drop are reported in Fig. 1. Both $\cos\Delta$ and $\tan\psi$ slowly increase, and then start to oscillate when one

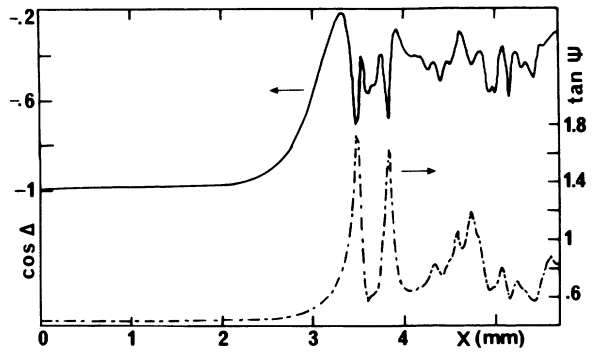

FIG. 1. Typical evolution of the two ellipsometric parameters cosΔ and tanψ along a drop radius, starting from distances very far from the drop center. Drop characteristics: PDMS of molecular weight $M_w = 6400$, volume $\Omega = 1.34 \times 10^{-5}$ cm^3.

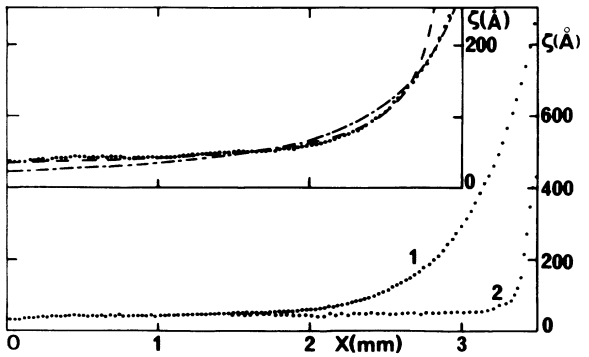

FIG. 2. Precursor film profiles obtained by spatially resolved ellipsometry on two PDMS drops of very different characteristics. Profile 1: $M_w = 6500$, $\Omega = 1.34 \times 10^{-5}$ cm^3, viscosity $\eta = 0.53$ P (Ref. 10), spreading time 75 h, $\theta_a = 0.055°$, $dR/dt\,|_{75\,h} = 1.8 \times 10^{-7}$ cm^2/sec, $\omega = 4.4 \times 10^{-9}$. Profile 2: $M_w = 280000$, $\Omega = 6.11 \times 10^{-7}$ cm^3, $\eta = 24500$ P (Ref. 10), spreading time 2856 h, $\theta_a = 0.914°$, $dR/dt\,|_{2856\,h} = 3.8 \times 10^{-10}$ cm^2/sec, $\omega = 4.2 \times 10^{-7}$. The two profiles are cut at the transition towards the macroscopic drop. In the inset (vertical scale expanded by 2) the dashed line is the best adjustment of the tail of profile 1 on the asymptotic form $z \sim a/[\omega(x - x_0)^\alpha]$ with $\alpha = 1$, while the dash-dotted line corresponds to $\alpha = 2$.

enters into the macroscopic drop where equal-thickness fringes can be observed through the microscope. The translation of cosΔ and tanψ data in terms of film thicknesses is a classical problem in ellipsometry. In a first approach, we have modeled our system by a one-dielectric layer of locally uniform thickness, treating the oxide layer (index of refraction $n = 1.45$) and the PDMS ($n = 1.43$) as the same optical medium. Ellipsometric data can then easily be inverted,[9] and the local film thickness obtained as a function of the distance through the drop. Even if classical, this inversion may be delicate: The film thickness is obtained through the argument of a complex number, X, root of a second-degree equation parametrized by cosΔ and tanψ. X has to be of modulus 1, a condition which allows one to choose between the roots, but its argument is only determined modulo 2π. In our case, starting from points very far from the macroscopic drop where the film thickness decays to zero, and then proceeding by continuity, yields the film's thickness without ambiguity, after subtraction of the oxide layer thickness, measured independently. Indeed, our getting $|X| = 1$ is a constraining test of the validity of the hypothesis of a locally uniform film. In the present experiments, the above procedure ceased to yield $|X| = 1$ as soon as the slope of the film surface became too large (typically of the order of 3×10^{-4} rad). We have chosen this criterion to locate, on each set of data, the transition towards the macroscopic drop, and checked visually that this point was indeed very close (within 10 or 20 μm) to the edge of the macroscopic drop as deduced from the location of the first black equal-thickness fringe.

In Fig. 2, what we think to be the first detailed determination of precursor film profiles formed during the spreading of nonvolatile liquids is reported for two PDMS drops of very different characteristics detailed in the figure caption. In both cases, a smooth and well-defined profile is clearly visible. Both the film thickness at the transition towards the macroscopic drop, and its lateral extension, are larger for the smaller θ_a value, in good qualitative agreement with the predictions of de Gennes and Joanny.[2,3] The thickness of the liquid very progressively decays to zero and we have not been able to detect the extremity of the film. This may be due to the residual roughness of the substrate (4 to 5 Å), not negligible in front of such a small thickness of the film.

Because of the good accuracy of the experimental profiles, more quantitative comparisons with theoretical predictions can be undertaken. The key points of the approach of de Gennes and Joanny are the following: (i) The range of the cohesive forces within the liquid is finite. The formation of a liquid slab of thickness e smaller than this range necessitates work against these forces, a contribution modeled by the disjoining pressure $\Pi(e)$ introduced by Deryagin.[11] (ii) If the liquid is not volatile, the only efficient spreading process is by flow of the liquid (no transport through the vapor phase). Thus, in the macroscopic drop, where the thickness is large compared with the range of the interactions, the driving force for the spreading is only related to the Laplace pressure due to the curved liquid-gas interface. Assumption of a Poiseuille-type flow in the advancing liquid edge leads to Tanner's laws[2,12] for $R(t)$ and $\theta_a(t)$. In particular, the velocity of the apparent macroscopic contact line, $V = dR/dt$, is proportional to θ_a^3: $\theta_a^3 \simeq (\eta/\gamma)V \simeq \omega$, with $\omega = \eta V/\gamma$ the capillary number, a relation well satisfied by all the drops we have studied (see Ref. 1). In contrast, the thin precursor film evolves under the action of both Laplace and disjoining pressure gradients. Again, the assumption of a Poiseuille-type flow leads, in a simple one-dimensional model, to a differential equa-

tion for the film profile:

$$\frac{3\eta V}{\zeta^2}=\frac{d}{dx}\left(-\gamma\frac{d^2\zeta}{dx^2}-\Pi(\zeta)\right), \quad (1)$$

with ζ the film thickness at the distance x from the macroscopic edge of the drop. If the explicit thickness dependence of Π is known [$\Pi(\zeta)\sim A/6\pi\zeta^3$, with A an effective Hamaker constant related to the polarizabilities of both the solid and the liquid, for nonretarded van der Waals interactions[2,13]] one is left with a highly nonlinear differential equation. For van der Waals interactions, Eq. (1) has a simple asymptotic solution, far from the macroscopic edge, where the curvature term $\gamma d^3\zeta/dx^3$, can be neglected:

$$\zeta(x)\sim a/\omega(x-x_0). \quad (2)$$

$a=(A/6\pi\gamma)^{1/2}$ has the dimension and the order of magnitude of a molecular length and x_0 is an integration constant to be determined by a suitable connection to the complete solution. The dashed line in Fig. 2 is the best least-squares fit of Eq. (2) to the 80 data points of the tail of profile No. 1, with a/ω and x_0 left as adjustable parameters. The agreement appears quite satisfactory. Adjustment of the full set of data on Eq. (2) was not possible. This is not too surprising as curvature terms may no longer be negligible close to the crossover towards the macroscopic drop. Slightly different analytical forms such as $\zeta\sim a/\omega(x-x_0)^\alpha$ have also been tried. The fit appears significantly better with $\alpha=1$ (the dash-dotted line in Fig. 2 corresponds to $\alpha=2$). Similar results have been deduced from profile No. 2, with a reduced accuracy as the film is less developed, and are not reported in the figure for clarity.

When the curvature of the free surface is not negligible, the full Eq. (1) has to be used. A numerical integration of Eq. (1) has been performed by Hervet and de Gennes,[14] after reduction to the dimensionless form

$$1=h'h^{-2}-h'''h^2, \quad (3)$$

with $\zeta=\zeta_0 h(y)$ and $x=x_0 y$. The scaling factors ζ_0 and x_0 depend on the actual parameters of the drop and are functions of a and ω only:

$$\zeta_0=3^{1/6}a\omega^{-1/3};\quad x_0=3^{-1/6}a\omega^{-2/3}. \quad (4)$$

Only one solution of (3) asymptotically recovers (2) for $y\to-\infty$ with a curvature going to zero for $y\to+\infty$ (connection to the macroscopic drop). We have tried to adjust our data on this solution called the "maximal film." We can estimate ω: $R(t)$ is measured, $\gamma\cong 22$ mN/m, and the viscosities deduced from the $\eta(M)$ data of Ref. 10 are reported in the caption of Fig. 2. We do not know a. We have thus used the following procedure to scale the data: Identification of the point $x=0$ (extremity of the macroscopic wedge, and point of maximum curvature in the numerical profile) with the point

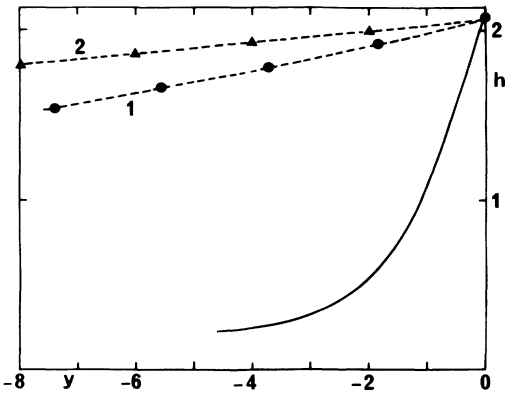

FIG. 3. Comparison of the experimental profiles of Fig. 2 with the numerical solution of Eq. (3) (full line), in the reduced dimensionless variable $h(y)$ calculated as detailed in the text. The experimental profiles develop much more rapidly than predicted, and the discrepancy is more pronounced for the larger molecular weight.

at which ellipsometric data can no longer be inverted fixes ζ_0, $\zeta(x=0)=\zeta_0 h(y=0)$ with $h(y=0)=2.08$.[14] Then a can be deduced from (4). For the two drops of Fig. 2, $\omega_{6400}=4.4\times10^{-9}$ and $\omega_{280000}=4.2\times10^{-7}$, and we get $a=0.5\pm0.05$ Å; both the order of magnitude and the agreement between the two different determinations are reasonable. x_0 can then be calculated. The scaled profiles of the two drops of Fig. 2 are reported in Fig. 3 along with the calculated maximal profile (continuous line). The agreement now appears quite poor. The two experimental profiles are far above the calculated one, and the situation is worst for the largest molecular weight.

Up to now, we have no definite explanation of this discrepancy. It could mean that the scaling procedure is incorrect. We are presently developing more elaborate inversion procedures for the ellipsometric data, taking into account the finite slope of the liquid-gas interface, from which the full profile (precursor film and macroscopic drop) will be determined. Anyhow, the transition to the macroscopic drop is sharp [the slope θ_a corresponds to a jump of 300 Å between two points for profile No. 1, and 3200 Å for profile No. 2 (in Fig. 2)], and the uncertainty of one x step in the position of the origin cannot by itself account for the differences between observed and calculated profiles.

In fact, the liquid we use is a high-molecular-weight polymer. In such liquids, molecular entanglements deeply influence the hydrodynamics,[15] and the boundary condition for the flow should rather be a finite velocity at the solid wall.[16,17] Brochard and de Gennes have studied the spreading behavior of a polymer drop in the presence of slippage[18]: (i) A foot, i.e., a zone with an upward curvature should appear in the thin regions of the macroscopic drop; (ii) the asymptotic law describing the precursor film far from the foot becomes $B(x-x_0)^{-1/2}$, two

characteristics not present in our experiments.

The precursor films we have characterized appear compatible with the simple liquid picture far from the drop, but have developed more rapidly than predicted by the approach of de Gennes and Joanny. This may mean that the driving forces are not correctly modeled by the simple van der Waals disjoining pressure, or that the viscosity (that we have assumed to be the bulk polymer viscosity) is not the correct one, especially when the thickness of the precursor film becomes smaller than the radius of gyration of the polymer chains which are thus partly disentangled.

Further systematic experiments varying the molecular weight are presently under way in order to test that last point. Direct characterizations of both the forces and the hydrodynamics at very short distances which are now possible,[13] performed on the same system (silica, PDMS), would strongly help in the understanding of the spreading process.

To conclude, we have, by ellipsometry, characterized the profile of the precursor films which slowly develop ahead of the macroscopic edge of spreading nonvolatile liquid drops, with both a high spatial (10 μm) and a high vertical (1 Å) resolution. These films qualitatively behave as predicted by Joanny and de Gennes: They are thicker and more extended when the apparent contact angle of the macroscopic drop is smaller. More quantitative comparisons, however, show that the predicted scaled form does not correctly describe the data. The films develop more rapidly than predicted, and the discrepancy is stronger for the larger molecular weight, a fact which may reveal specific polymeric effects.

Physique de la Matière Condensée is Unité Associé No. 792 au Centre National de la Recherche Scientifique. Electronique et Physique Appliquée is a member of the Philips Research Organization.

[a]Present address: IBM Research, Almaden Research Center, 650 Harry Road, San Jose, CA 95120.

[1]D. Ausserre, A. M. Picard, and L. Leger, Phys. Rev. Lett. **57**, 2671 (1986).

[2]P. G. de Gennes, Rev. Mod. Phys. **57**, 827 (1985).

[3]J. F. Joanny, thesis, Université Paris VI, 1985 (unpublished).

[4]The characterization of our system by x-ray reflectivity has been performed by J. J. Benattar, F. Rieutord, and L. Bosio, unpublished.

[5]M. Pomeratz, A. Segmüller, L. Netzer, and J. Sagiv, Thin Solid Films **132**, 153 (1985).

[6]J. R. Vig, J. Vac. Sci. Technol. A **3**, 1027 (1985).

[7]M. Erman and J. B. Theeten, J. Appl. Phys. **60**, 859 (1986).

[8]M. Erman, thesis, Université Paris VI, 1986 (unpublished).

[9]R. M. A. Azzam and N. M. Bashara, *Ellipsometry and Polarized Light* (North-Holland, Amsterdam, 1977).

[10]The viscosities have been estimated by extrapolation of the $\eta(M_n)$ data of R. R. Rahalker *et al.*, Proc. Roy. Soc. London A **394**, 207 (1984).

[11]B. Deryagin, Zh. Fiz. Khim, **14**, 137 (1940).

[12]L. Tanner, J. Phys. D **12**, 1473 (1979).

[13]J. N. Israelashvili, *Intermolecular Forces* (Academic, New York, 1985), Chap. 6.

[14]H. Hervet and P. G. de Gennes, C.R. Acad. Sci. Ser. 2 **299**, 499 (1984).

[15]For a review on the dynamic properties of entangled systems, see W. W. Graessley, Faraday Symp. Chem. Soc. **18**, 315 (1983).

[16]P. G. de Gennes, C.R. Acad. Sci. Ser. B **298**, 219 (1979).

[17]R. H. Burton, M. J. Folkes, K. A. Narh, and A. Keller, J. Mater. Sci. **18**, 315 (1983).

[18]F. Brochard and P. G. de Gennes, J. Phys. Lett. **45**, L597 (1984).